

# Numerical Simulation of Wave-Structure Interaction using Eulerian and Lagrangian CFD Methods

Jan Westphalen<sup>1</sup>, Deborah Greaves<sup>1</sup>, Alison Hunt-Raby<sup>1</sup>, Chris Williams<sup>2</sup>, Paul H. Taylor<sup>3</sup>, Zheng Zheng Hu<sup>4</sup>, Pourya Omidvar<sup>5</sup>, Derek Causon<sup>4</sup>, Clive Mingham<sup>4</sup>, Peter K. Stansby<sup>5</sup>, Benedict D. Rogers<sup>5</sup>, Tim Stallard<sup>5</sup>

<sup>1</sup>PRIMaRE: Peninsula Research Institute for Marine Renewable Energy,  
Department of Marine Science and Engineering,  
University of Plymouth,  
Drake Circus, Plymouth, PL4 8AA, UK  
E-mail: jan.westphalen@plymouth.ac.uk

<sup>2</sup>Department of Architecture and Civil Engineering,  
University of Bath,  
Bath, BA2 7AY, UK

<sup>3</sup>Department of Engineering Science,  
University of Oxford,  
Parks Road,  
Oxford, OX1 3PJ, UK

<sup>4</sup>Department of Computing and Mathematics,  
Manchester Metropolitan University,  
Chester Street,  
Manchester, M1 5GD, UK

<sup>5</sup>School of Mechanical, Aerospace and Civil Engineering,  
University of Manchester,  
Manchester, M60 1QD, UK

## Abstract

Three mesh methods, solving the Navier-Stokes and the Euler equations, and a SPH method are applied to two fluid-structure interaction problems including rigid body motion.

The first test case concerns the simulation of the forced motion of a cone-shaped body close to the water surface. Here, the vertical fluid force and the surface motion close to the cone are compared with physical experiments.

The second test case is directly related to the simulation of a wave energy converter. A single floating body in extreme waves is modelled in one degree of freedom. Furthermore the interaction between the float and a counterweight, which is connected to it by a rope-pulley system, is taken into account. The vertical translations of the floating body are compared to measured results from physical tank tests.

**Keywords:** AMAZON, CFX 11, floating body, Oscillating cone, STAR CCM+, SPhysics, wave-structure interaction

## 1 Introduction

Recent climate changes make it necessary to access alternative energy resources, which are CO<sub>2</sub> neutral in their emissions. Thus offshore wave energy has drawn a lot of attention and research interest, as it has the potential to contribute to low-carbon energy strategies significantly. Besides making the wave energy converters efficient in average sea states for which they are optimised in the first place, the other important design consideration concerns the survivability in extreme seas, such as occurred with the New Year wave at the Draupner platform in the North Sea.

Within the EPSRC funded research project “Extreme Wave Loading on Offshore Wave Energy Devices: a Hierarchical Team Approach” the two WECs, Pelamis and the Manchester Bobber, are investigated regarding their survivability. Two test cases leading towards the simulation of the full dynamics of Pelamis and the Manchester Bobber have been modelled using different Eulerian and Lagrangian CFD techniques. The problems involve the hydrodynamics an oscillating cone near the still water surface. Results are compared with experimental data to calibrate the CFD codes. Furthermore, results are presented for fluid-structure interaction will include a floating cylinder representing

a float of the Manchester Bobber in extreme focused waves using NewWave theory. These are compared with tank tests, which were carried out during the design of the Manchester Bobber.

Four different CFD codes are applied to simulate the test cases: Smoothed Particle Hydrodynamics, a Cartesian Cut Cell method based on an artificial compressibility method with shock capturing for the interface, and two pressure-based Navier-Stokes codes, one using a Finite Volume and the other a control volume based Finite Element approach.

## 2 Numerical Methods

The **Finite Volume (FV)** solver uses the Navier-Stokes equations discretised on a 3-dimensional mesh to calculate the velocities and pressures in the flow field in a segregated iterative way. The variables are collocated on the grid and the flow is assumed incompressible.

The domain, here a numerical wave tank (NWT) including the structure, i.e. the cone shaped body and the float, is subdivided into discrete volumes. The surface and volume integrals of the discretised equations are performed on the control volumes to calculate the primitive variable values such as the fluid velocities and pressures at the centre node of each control volume (CV). This approach makes the Finite Volume method conservative by construction. Calculations are performed for both fluids, i.e. water and air, using the well known Volume of Fluid (VoF) method. For the CVs containing the fluid interface a high resolution interface capturing scheme, described by [1-3] is applied.

The **control-volume Finite Element (CV-FE)** approach combines the Finite Volume method considering the control volumes and the Finite Element method by using shape functions and a different discretisation scheme. The shape functions are used to calculate the change of a variable across the CV. [4-6] As described for the Finite Volume method, the CV-FE also solves the Navier-Stokes equations for incompressible fluids. The general transport equation is discretised on a 3-dimensional grid containing hexahedral cells. The CVs are arranged around the mesh nodes and thereby this technique ensures the conservation of flow quantities such as mass and momentum.

In all simulations the fluid fractions of air and water are solved using the Volume of Fluid formulation. The fluid interface is treated by the method described by [4-7] which is dependent on the filling level of the surrounding cells rather than the Courant number as in [1]. This solver is used for the oscillating cone.

**Smoothed Particle Hydrodynamics (SPH)** is a flexible Lagrangian technique for computational fluid dynamics simulations. In this method the fluid system is represented by a set of particles which have individual material properties and move according to governing conservation equations [8]. There is no mesh

construction in SPH, therefore in certain problems, for instance simulation of waves, the SPH method may be easier to develop and use than Eulerian methods.

To simulate water, the fluid is allowed to be weakly compressible using an artificial equation of state described by [8] so that the time step is not prohibitively small. The simulations are run using the open source code SPHysics [9]. The symplectic algorithm described by [10], often known as kick-drift-kick, is used as the time stepping method. The governing equations for compressible Navier-Stokes flow written in SPH form include position, conservation of mass and momentum and are described by [11]. The interaction between each particle pair is solved as a Riemann problem for velocity, pressure and density. The scheme is rendered second-order accurate using TVD reconstruction and there is no explicit viscosity formulation in the model.

The repulsive boundary condition, developed by [12] and modified by [13], is used which prevents a water particle crossing a solid boundary. This technique is used to simulate the oscillating cone case. By the principle of equal and opposite reaction, the forces on the structure can be estimated by summing the forces exerted on the body particles by water particles.

The **AMAZON-3D** numerical wave tank (NWT) for the study of wave loading on a wave energy converter (WEC) device has been developed at MMU, which is based on the free-surface capturing method for two fluid flows with moving bodies developed by [14, 15], which demonstrated a rigid 2D wedge shaped body entering calm water and its subsequent total immersion. The NWT, based on a two fluid free surface capturing and Cartesian cut cell method, is being developed for the simulation of wave loadings on the Manchester Bobber and Pelamis devices under extreme wave conditions.

The AMAZON-3D code uses a Cartesian cut cell method to provide a boundary-fitted grid for both static and moving boundaries in 3D. The main advantages of the Cartesian cut cell approach have been outlined previously by [16, 17], including particularly its flexibility for dealing with complex geometries and moving bodies. There is no requirement to re-mesh globally or even locally for a moving boundary problem which only requires changes locally at cells in the background Cartesian mesh that are cut by the moving boundary contour. The AMAZON-3D code has been extended to handle a 3D floating bobber moving in the vertical direction in extreme waves. Also for this paper the code is applied to the simulation of a cone shaped body, which oscillates at the water surface.

The AMAZON-3D code is based on the integral form of the Euler equations for 3D incompressible flow with variable density. The free surface is treated as a contact surface in the density field that is captured automatically during a time-marched calculation without special provision in a manner analogous to shock capturing in compressible flow. A time-accurate artificial compressibility method and high resolution Godunov-type scheme replace the pressure correction

solver used in many current VoF methods. AMAZON-SC can handle break-up and recombination of the free surface as well as air entrainment into the water and, in principle, associated local compressibility effects. The total force is obtained by integration of the pressure field along the body.

### 3 Oscillating Cone at Still Water Surface

For the simulation of floating bodies, the authors' main interest lies in Pelamis and the Manchester Bobber, so it is important to be able to calculate the forces on a moving body and the surface elevations around it correctly. For the purpose of the validation of the codes a simplified test setup accommodating a cone shaped body near the water surface is chosen. The motion of the cone is driven and not influenced by the forces generated on its surface by the surrounding fluids. The physical tank tests are described in [18]. In the experiments, the vertical forces on the cone surface due to its motion and the relative water surface elevation at a distance of 0.02m from the cone surface were recorded. Here comparisons between AMAZON, the CV-FE solver, SPHysics and the physical experiments are shown.

The motion of the cone is defined by the displacement  $d(t)$  from the initial position at  $t = 0s$  following the form of a Gaussian wave packet, which is described by

$$d(t) = A \sum_{n=1}^N Z(\omega_n) \cos \left[ \omega_n (t - t_0) - \frac{h\pi}{2} \right] \Delta \omega_n \quad (1)$$

where

$$Z(\omega_n) = \frac{1}{\frac{\omega_n}{2\pi} \sqrt{2\pi}} \exp \left[ -\frac{(\omega_n - \omega_0)^2}{2 \left( \frac{\omega_0}{2\pi} \right)^2} \right] \quad (2)$$

with  $h = 0$  or  $1$ .  $A$  denotes the largest excursion from the still water level.  $N$  is the number of frequency components and  $\omega_n$  is the appropriate circular frequency. The central circular frequency  $\omega_0$  [rad/s] is defined by

$$\omega_0 = \frac{m\pi}{3} \quad (3)$$

with  $m$  being an integer between 1 and 12.

For the CV-FE approach the simulations are performed in a three-dimensional domain with a length and width of 2.5m and a height of 2.0m. The cone is placed in the centre, as can be seen in Figure 1 and has a top diameter of 0.6m and a deadrise angle of 45°. The slope itself is 0.3m high. The initial draught of the cone is 0.15m at a water depth of 1.0m. The cone is modelled as a cavity in the mesh. The outer boundaries, the bottom and the cone are modelled as free slip walls. The top boundary is defined as a pressure outlet with constant atmospheric pressure. The mesh consists of 820,000 hexahedral cells, where the regions around the water surface and the cone surface are highly refined to achieve cell edges of approximately 0.01m. The outer regions are relatively

coarse to save computational resources and encourage numerical damping, thus avoiding reflections from the walls. The simulations were carried out using high performance computing on 16 CPUs. The timestep is 0.0005s.

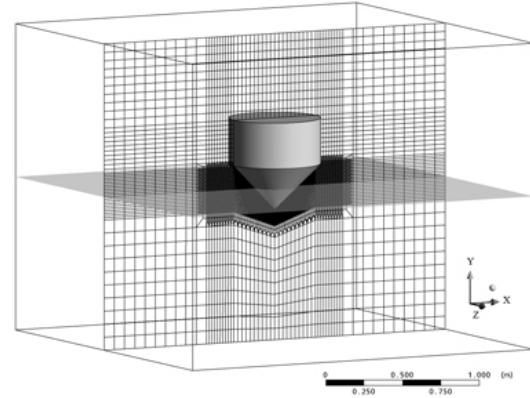


**Figure 1: Domain with cone at initial water surface used for the CV-FE simulations**

For the AMAZON simulations a 2m x 1.6m axisymmetric domain is used. The still water level is set to 1.02m and the initial draught of the cone is 0.148m. The calculations are performed on a hexahedral grid using an axisymmetric (2D) version of the code with cell sizes of 0.02 x 0.02m. The timestep is 0.0005s.

The exported vertical forces  $F_z$  from the CFD codes are non-dimensionalised using the expression

$$F'(t) = \frac{F_z(t)}{\rho g \pi r^2 A} \quad (4)$$

with  $\rho$  being the density of fresh water,  $g$  the acceleration due to gravity,  $r$  the cone radius at still water level and  $A$  the maximum excursion. Also the time is divided by the corresponding period of the central frequency  $\omega_0$ . The measured relative motion of the water surface is divided by the maximum excursion  $A = 0.05m$ .

Figure 2 compares the force data obtained by the three CFD methods with those of the physical experiment. Generally the agreement is satisfactory. The Eulerian techniques generate little differences especially in the force minima and maxima. AMAZON slightly overestimates the forces and the Navier-Stokes solver underestimates them. The Lagrangian SPH method also agrees well although the troughs are less well resolved. Further results regarding the surface elevation around the cone will be presented on the conference.

For the solution of the relative motion of the free surface at the cone, shown in Figure 2, the differences become larger for the mesh techniques. Here, AMAZON and the CV-FE code generate results, which are smaller in the crests and larger in the troughs. The SPH results agree very well with the physical experiments. The difficulty with capturing the free surface close to the cone is due to the occurrence of a jet-effect. This is not apparent for cone cases with low central frequency, where the relative motion of the

surface elevation is resolved better. These results will be presented at the conference and are described by [19, 20].

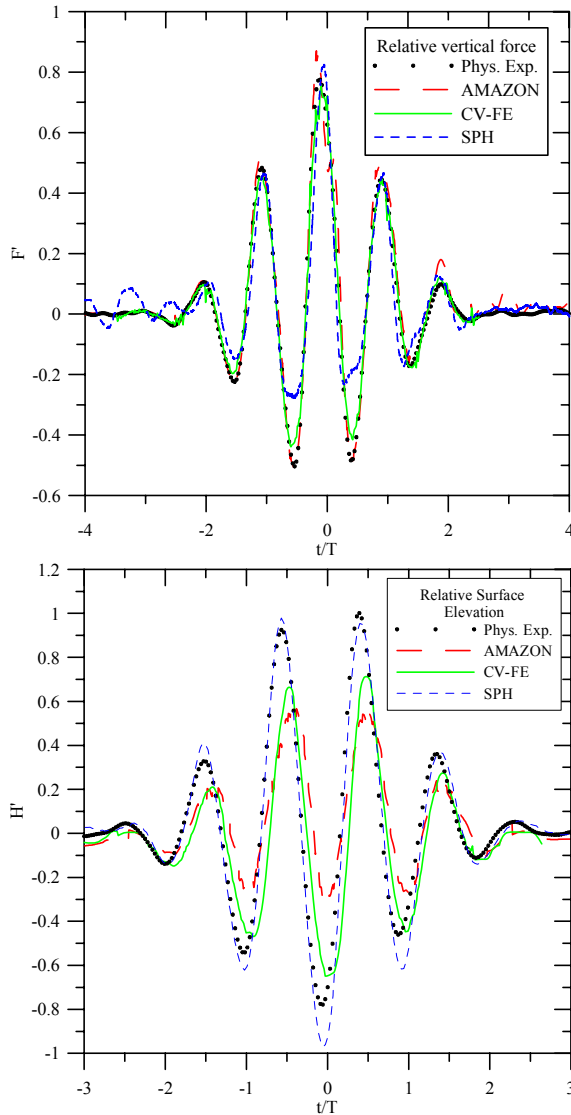


**Figure 2: Forces (top) on cone surface and surface elevation around cone ( $m = 9$  and  $A = 0.05$  m)**

#### 4 Floating Body in Extreme Waves

The physical tank tests were performed in the wavetank of the University of Manchester. It is 18.5 m long, 5 m wide and tests were done with a water depth of 0.5 m. The waves are generated using 8 piston type paddles operated using the Edinburgh Designs “OCEAN” interface. To minimise reflections from the far end wall, a curved surface piercing beach is installed.

Here, tests for a single tethered float (see Figure 3) are reproduced using the AMAZON and the FV solvers. A schematic arrangement of the system can be seen in Figure 4a, where  $m_f$  and  $m_c$  are the masses of the float and the counterweight respectively. The horizontal displacement of the float is restricted due to the vertical cables. These are attached to the superstructure and held taut by weights at their ends. In

the physical experiments vertical displacements are deduced from the angular displacement of the pulley  $\omega_p$ . During all tests no power was taken off the system and the friction in the pulley support is negligible. The cables are assumed to be stiff and inextensible. Further details on the experimental system are given by [21] for a different float form and mass.

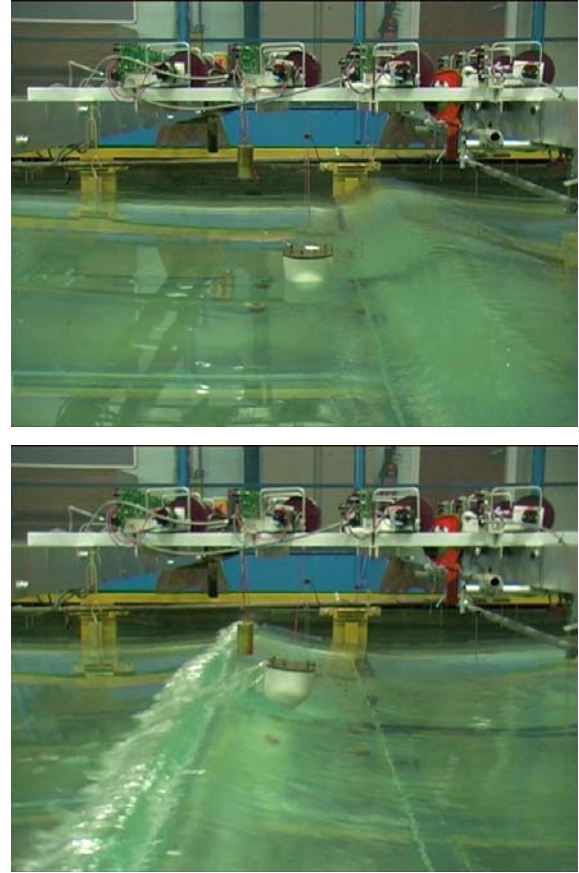


**Figure 3: Physical tank test of single tethered float in extreme wave [22]**

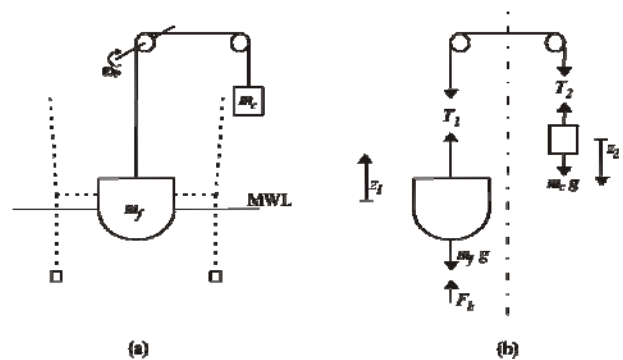


**Figure 4: Mechanical system (a) and free body diagram (b) of single float experiments**

For the simulation of the mechanical system in CFD it is necessary to know the relationship between the two accelerated bodies, i.e. the float and the counter weight. The reason for this is that the CFD code cannot model the pulley system and the counter weight directly, and so these are approximated using additional body forces. The free body diagram as seen in Figure 4b is used to



find the unknown tension forces in the cable  $T_1$  and  $T_2$  and the acceleration of the system.

The two unknowns of the system, such as the acceleration of the float and the tension force  $T$  can then be written as

$$\ddot{z} = \frac{(m_c - m_f)g + F_b}{m_f + m_c} \quad \text{and} \quad T = -m_c \frac{(m_c - m_f)g + F_b}{m_f + m_c} + m_c g \quad (5a,b)$$

In the computational approach  $F_b$  is calculated from the integrated pressures on the float surface and thereby known at any time. For the numerical simulations NewWave focussing is used to generate the extreme wave [23]. The concept of wave focusing is to generate several waves of relatively small amplitudes and different periods. These waves interact and constructive interfere to build up a localised extreme wave, larger than any individual wave created at the paddle, focused at a specified position and time in the tank.

For each wave component  $n$  the amplitude  $a_n$  is defined as

$$a_n = A \frac{S_n(f) \Delta f}{\sum_n S_n(f) \Delta f} \quad (6)$$

where  $S_n(f)$  is the spectral density,  $\Delta f$  is the frequency step depending on the number of wave components and bandwidth and  $A$  is the target linear amplitude of the focused wave. Thus, the amplitude of every spectral component in the NewWave group scales as the power density within that frequency band in the assumed sea-state. Equivalently, NewWave is simply the scaled auto-correlation function corresponding to a specified frequency spectrum such as the one obtained on the measured surface elevation time history at the location of the float without the float being in place during the physical tank tests.

The waves are generated using a velocity inlet at the left hand boundary of the numerical wave tank (NWT) at  $x = 0$ . Here, the surface elevation of the wave group is prescribed using equation (7) by specifying the vertical location of the water volume fraction of 0.5, which is taken to represent the fluid interface between water and air. For the water fraction at the inlet the horizontal and vertical velocity components coming from NewWave theory and given by equations (8) and (9) are applied. The equations are first order accurate and described by

$$\eta^{(1)} = \sum_{i=1}^N a_i \cos(k_i x - \omega_i t + \epsilon_i) \quad (7)$$

$$u^{(1)} = \sum_{i=1}^N \frac{a_i k_i g}{\omega_i} \frac{\cosh k_i(z+h)}{\cosh k_i h} \cos(k_i(x-x_0) - \omega_i(t-t_0) + \epsilon_i) \quad (8)$$

and

$$w^{(1)} = \sum_{i=1}^N \frac{a_i k_i g}{\omega_i} \frac{\sinh k_i(z+h)}{\cosh k_i h} \sin(k_i(x-x_0) - \omega_i(t-t_0) + \epsilon_i) \quad (9)$$

$a_i$  denotes the wave height for each wave component  $i$  as given in equation (6),  $k$  is the wavenumber,  $\omega$  is the angular frequency,  $t$  the time and  $\epsilon$  the phase angle, which is 0 for all calculations.  $t_0$  and  $x_0$  are the chosen focus time and location in the tank, here set to 4.6 s and 3.5 m respectively.  $N$  is the number of wave components, here 15.

The numerically reproduced wave without the float in place using AMAZON and the FV solver can be seen in Figure 5.

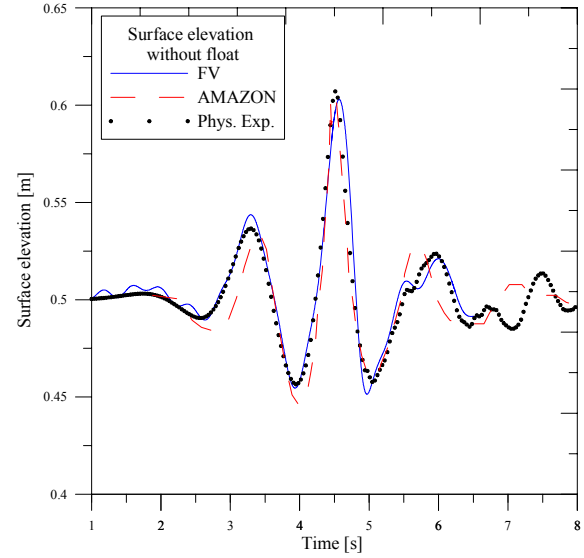


**Figure 5: Surface elevation at location of float without the float being in place; left: AMAZON, right: FV solver**

The difficulty for this case is the interaction of the float with the extreme wave, but also its interaction with the connected counterweight. Therefore the test series as outlined in Table 1 is conducted. First the numerical setup is simplified by subtracting the mass of the counterweight from the mass of the float and thereby neglecting the inertia of the counterweight (Case A). Then the mass of the float in the numerical experiment is increased to the same value as in the physical experiment and an additional vertical body force representing the pulley-counterweight system is included (Case B). Finally the full expression for the vertical body force as derived in equation (5a,b) is included (Case C).

The results are shown in Figure 6. Due to the reduced inertia in the system the float in the numerical simulations of Case A do not oscillate as the float in the physical experiment does. With the constant upward body force included (Case B) the displacement of the numerically simulated float is in reasonable agreement with the translation measured in the physical experiment. Case C, where the full expression according to equation (5a,b) is used significantly overestimates the displacement of the float

## 5 Conclusions

Four CFD methods were applied to two test cases involving rigid body motion. The first case was the prescribed motion of a cone shaped body close to the water surface, where the forces on the structure and the relative motion of the water surface were recorded and compared with physical experiments. Here the AMAZON-SC, the CV-FE solver and SPH all gave good results, although differences in the numerical results especially in the trough and crests of the force and surface elevation time histories could be identified.

The second case is directly related to wave energy conversion. Here, the displacement of a single degree-of-freedom floating body in extreme focused waves is modelled. The float interacts with the waves, but also with a counterweight, which is represented by a body force in the CFD approaches. The complexity of the numerical representation is increased in the progression of the CFD test series by first neglecting the counterweight, then adding only the gravitational term of the counterweight and finally using the full expression as given in equation (5a,b) for the tension force neglecting cable extension. Without the inertia of the counterweight the vertical motion of the float damps out immediately after the waves have passed the body. With the constant upward force included (Case B), the vertical displacement in the CFD simulations is in very good agreement to the physically measured results. Slight differences in the magnitude and phase of the oscillations can be observed. These are believed to occur because the tension force does not include the varying part of equation (5a,b). However, when including the full term to the tension force (Case C), the FV solver significantly overestimated the displacements. This effect is under investigation and further results will be presented on the conference.

From previous investigations and the results presented here, the overall performance of all four codes is found to be good. With sufficient computing power and being applied accordingly to their requirements, the codes are a very powerful supplement to tank testing in the design process of offshore structures and wave energy converters in particular.

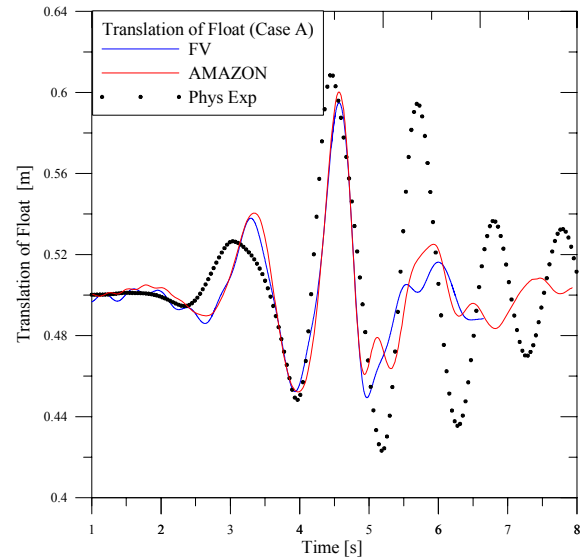


Figure 6. Translation of Float (Case A)

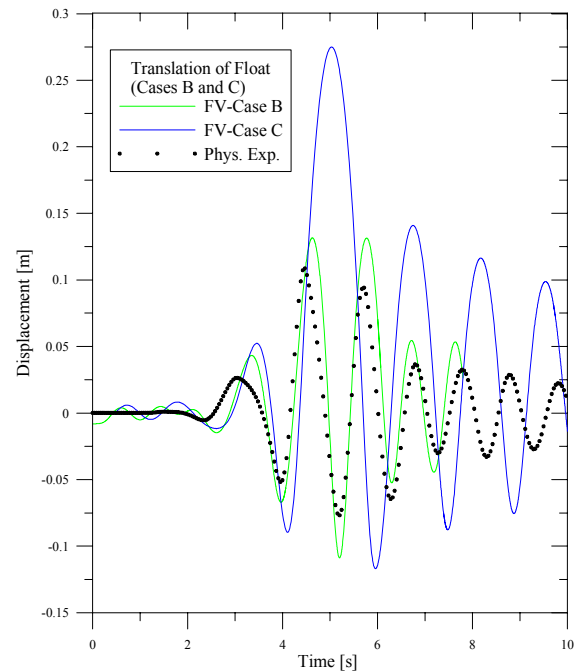


Figure 7: Translation of Float (Cases B and C)

Table 1: Properties of single float simulation

	A	B	C
Mass of float	$m_f - m_c$	$m_f$	$m_f$
Vertical Force	-	$m_c * g$	$m_c * g - m_c * zddot$
Solvers	FV/AMAZ	FV	FV

## Acknowledgements

The authors would like to thank Dr. Kevin Drake from the University College London for providing the high quality physical test data used for the cone simulations.

The work was funded by the Engineering and Physical Science Research Council under the project

title "Extreme Wave Loading on Offshore Wave Energy Devices using CFD: a Hierarchical Team Approach" (Grant No. EP/D077508).

## 6 References

- [1] Ubbink, O. (1997). Numerical prediction of two fluid systems with sharp interfaces. Department of Mechanical Engineering. London, Imperial College of Science, Technology & Medicine. PhD: 138.
- [2] Ferziger, J. H. and Peric, M. (2001). Computational Methods for Fluid Dynamics Heidelberg, Springer.
- [3] CD-Adapco (2009). STAR CCM+ Version 4.04.011. London, UK.
- [4] Zwart, P. J., Scheuerer, M. and Bogner, M. (2003). Free Surface Modelling of an Impinging Jet. *ASTAR International Workshop on Advanced Numerical Methods for Multidimensional Simulation of Two-Phase Flow*, Garching, Germany.
- [5] Zwart, P. J. (2005). Numerical Modelling of Free Surface and Cavitating Flows. *VKI Lecture Series*, Ansys Canada Ltd.: 25.
- [6] Ansys, I. (2006). ANSYS CFX-Solver Theory Guide. Canonsburg, USA.
- [7] Barth, J. T. and Jespersen, D. C. (1989). The Design and Application of Upwind Schemes on Unstructured Meshes. AIAA, Reno/Nevada.
- [8] Monaghan, J. J. (2005). "Smoothed particle hydrodynamics." *Reports on Progress in Physics* 68(8): 1703-1759.
- [9] SPHysics. (2010). "<http://wiki.manchester.ac.uk/sphysics>."
- [10] Leimkuhler, B. J., Reich, S. and Skeel, R. D. (1994). Integration methods for molecular dynamics. *Mathematical Approaches to Biomolecular Structure and Dynamics*, IMA Volumes in Mathematics and its Applications, Springer: 161-185.
- [11] Vila, J. P. (1999). "On Particle Weighted Methods and Smoothed Particle Hydrodynamics." *Mathematical Models and Methods in Applied Sciences* 28(3): 395-418.
- [12] Monaghan, J. J. and Kos, A. (1999). "Solitary waves on a cretan beach " *Journal of Waterway, Port, Coastal and Ocean Engineering* 125(8): 145-154.
- [13] Rogers, B. D. and Dalrymple, R. A. (2008). SPH modelling of tsunami waves. *Advances in Coastal and Ocean Engineering*, Vol 10 Advanced Numerical Models for Tsunami Waves and Runup. W. Scientific.
- [14] Qian, L., Causon, D. M., Mingham, C. G. and Ingram, D. M. (2006). A free surface capturing method for two fluid flows with moving bodies. *Proceedings of the Royal Society A: Mathematical, Physical and Engineering Science*. 462: 21-42.
- [15] Qian, L., Mingham, C. G., Causon, D. M., Ingram, D. M., Folley, M. and Whittaker, T. (2005). "Numerical simulation of wave power devices using a two-fluid free surface solver." *Modern Physics Letters B* 19(28&29): 1479-1482.
- [16] Causon, D. M., Ingram, D. M. and Mingham, C. G. (2001). "A cartesian cut cell method for shallow water flows with moving boundaries." *Advances in Water Resources* 24(8): 899-911.
- [17] Causon, D. M., Ingram, D. M., Mingham, C. G., Yang, G. and Pearson, R. V. (2000). "Calculation of shallow water flows using a Cartesian cut cell approach." *Advances in Water Resources* 23: 17.
- [18] Drake, K. R., Eatock Taylor, R., Taylor, P. H. and Bai, W. (2008). "On the hydrodynamics of bobbing cones." *Ocean Engineering* 36: 1270-1277.
- [19] Westphalen, J., Greaves, D. M., Williams, C. J. K., Drake, K. and Taylor, P. H. (2009). Numerical simulation of an oscillating cone at the water surface using computational fluid dynamics. *24th International Workshop on Water Waves and Floating Bodies*, St. Petersburg, Russia.
- [20] Westphalen, J., Greaves, D. M., Williams, C. J. K., Taylor, P. H., Causon, D. M., Mingham, C. G., Hu, Z. Z., Stansby, P. K., Rogers, B. D. and Omidvar, P. (2009). Extreme wave Loading on Offshore Wave Energy Devices using CFD: a Hierarchical Team Approach. *European Wave and Tidal Energy Conference*, Uppsala, Sweden.
- [21] Stallard, T., Weller, S. D., Stansby, P. K. (2010). Limiting heave response of a wave energy device by draft adjustment and upper surface immersion. *Applied Ocean Research*. In press.
- [22] Stallard, T. and Stansby, P.K (2009). Personal communication.
- [23] Taylor, P. H. and Williams, B.A. (2004). "Wave Statistics for Intermediate Depth Water - NewWaves and Symmetry." *Journal of Offshore Mechanics and Arctic Engineering* 126: 6.